

Effects of Particle Surface Areas and Microstructures on Photocatalytic H₂ and O₂ Production over PbTiO₃

David Arney, Tylan Watkins and Paul A. Maggard[†]

Department of Chemistry, North Carolina State University, Raleigh, North Carolina 27695-8204

The visible-light photocatalyst PbTiO₃ was prepared in molten NaCl and PbO fluxes using 0.5:1–20:1 flux-to-reactant molar ratios by heating to 1000°C for a duration of 1 h. Yellow-colored powders were obtained in high purity, as confirmed by powder X-ray diffraction and exhibited a bandgap size of ~2.75 eV as determined by UV–Vis diffuse reflectance measurements. Roughly spherical and cubic shaped particles with homogeneous microstructures were observed with sizes ranging from ~100 to 6000 nm, and surface areas ranging from 0.56 to 2.63 m²/g. The smallest particle-size distributions and highest surface areas were obtained for the 10:1 NaCl flux molar ratio. By comparison, solid-state preparations of PbTiO₃ particles exhibit no well-controlled sizes or microstructures. The water-splitting photocatalytic activities of the PbTiO₃ particles were evaluated in visible light ($\lambda > 420$ nm), and yielded maximum rates of 27.4 $\mu\text{mol} \cdot \text{H}_2 \cdot (\text{g} \cdot \text{h})^{-1}$ for the PbTiO₃ prepared using a 1:1 PbO molar ratio and 183 $\mu\text{mol} \cdot \text{O}_2 \cdot (\text{g} \cdot \text{h})^{-1}$ for the solid-state prepared sample. The rates were inversely correlated with the particle surface areas. The relationship between particle morphology and photocatalytic activity provides important insights into understanding the origins of photocatalysis in metal-oxides.

I. Introduction

SYNTHESIS of new metal-oxide materials for the photocatalytic production of hydrogen and oxygen from water has had remarkable and rapid growth over the past 25 years.^{1–5} Recently, intense research efforts have been made by several groups to utilize the largest fraction of the solar spectrum and to develop working visible-light active photocatalysts for the overall splitting of water.^{6–11} In particular, particle sizes and surface morphologies have been shown to significantly contribute to the performance of the photocatalyst.^{12–15} It has been reported that Pb²⁺-containing early transition-metal oxides (e.g., Nb, Ta, Ti) can absorb light in the visible range due to their smaller bandgap sizes.^{16,17} This arises because of higher energy Pb 6s orbitals that mix with the O 2p valence band orbitals, and which are still sufficiently below the oxidation potential of H₂O. Among these examples, PbTiO₃ is a recently reported visible-light active photocatalyst and known ferroelectric with a bandgap size of ~2.75 eV.¹⁷ However, the preparation of PbTiO₃ in previous studies proceeded via traditional solid-state synthesis, and which provides little control of the particle size and surface characteristics that could significantly affect their photocatalytic activity. As an alternative method, the utilization of molten-salt flux techniques has shown the capability to help better modulate particle sizes and surface features, and which can provide a deeper understanding of how the surfaces influence these reactions.^{18–20} Also, the use of molten-salt flux techniques for the preparation of

metal oxides can enable shorter reaction times and reduced reaction temperatures.^{21–27}

Presented herein is an investigation of the visible light photocatalytic properties of ferroelectric PbTiO₃ particles prepared via molten-salt flux methods in order to determine the role of particle size and surface morphology on its photocatalytic activities. The flux synthesis of PbTiO₃ has been previously reported in the literature based on the use of alkali metal salts.^{28,29} However, the research motivation herein was to investigate the photocatalytic activities of flux-prepared PbTiO₃ powders as a function of synthetic conditions and in comparison to their solid-state prepared counterparts. The PbTiO₃ particles were synthesized within molten NaCl and PbO using different flux-to-reactant ratios, followed by an investigation of its effect on the particle sizes and morphologies, as well as their optical properties and photocatalytic rates for H₂ and O₂ formation. The products were characterized by powder X-ray diffraction (PXRD), UV–Vis diffuse reflectance spectroscopy (DRS), BET surface-area analysis, field-emission scanning electron microscopy, and their photocatalytic activities for H₂ and O₂ production.

II. Experimental Procedure

(1) Synthesis and characterization

The flux synthesis of PbTiO₃ was performed by combining a stoichiometric mixture of PbO (Alfa Aesar, 99.99%) and TiO₂ (Alfa Aesar, Ward Hill, MA; Anatase, 99.9%) and grinding it in acetone for 30 min before the addition of either the NaCl (melting point = 801°C) salt flux in flux-to-reactant molar ratios of 1:1, 10:1, and 20:1, or the PbO (melting point = 888°C) flux in molar ratios of 0.5:1, 1:1, and 2:1. After grinding, the reactant mixtures were then placed inside alumina crucibles and heated to 1000°C inside a box furnace in air for a reaction time of 1 h. The crucibles were allowed to radiatively cool to room temperature inside the furnace. The resulting powders were washed with hot deionized water to remove the flux, and then washed briefly in 1M HNO₃ to remove excess PbO flux and then dried overnight in an oven at 80°C. Fine homogeneous yellow powders of PbTiO₃ were obtained in high purity, as judged from PXRD. The solid-state method of preparing PbTiO₃ involved grinding, pelletizing, and heating the stoichiometrically combined PbO and TiO₂ reactants at 1000°C for 48 h, according to the reported procedures.¹⁷

High-resolution PXRD data of all products were collected on an INEL diffractometer using CuK α_1 ($\lambda = 1.54056$ Å) radiation from a sealed-tube X-ray generator (35 kV, 30 mA) using a curved position sensitive detector (CPS120). Unit cell parameters of the flux-prepared samples were calculated using the LATCON software program.³⁰ Field-emission scanning electron microscopy analyses were performed on a JEOL SEM 6400, (Peabody, MA) and concomitantly the energy dispersive X-ray (EDX) spectra were taken as a check of the elemental compositions. UV–Vis diffuse reflectance spectra (DRS) were collected for all samples on a Shimadzu UV-3600 spectrophotometer (Shimadzu, Columbia, MA) equipped with an integrating sphere. BET surface area analyses were performed using a

Prof. G. S. Rohrer—contributing editor

Manuscript No. 28354. Received July 26, 2010; approved October 15, 2010.

[†]Author to whom correspondence should be addressed. e-mail: paul_maggard@ncsu.edu

Quantachrome ChemBET Pulsar TPR/TPD (Quantachrome, Boynton Beach, FL).

(1) Photocatalysis Testing

The photocatalytic activity for either H_2 or O_2 formation were carried out separately using an outer-irradiation type fused-silica reaction cell with a volume of 90 mL and irradiated under both ultraviolet ($\lambda > 300$ nm) and visible ($\lambda > 420$ nm) light energies. For the photoreduction of H^+ to H_2 , each sample was first loaded with a 1 wt% Pt cocatalyst using the well-known photo-deposition method.⁵ Numerous previous studies have shown that platinum islands on a metal oxide surface can function as a kinetic aid for the reduction of H^+ to give H_2 .³¹ Typically, 200 mg of a $PbTiO_3$ sample was mixed with 30 mL of an aqueous solution of dihydrogen hexachloroplatinate(IV) ($H_2PtCl_6 \cdot 6H_2O$; Alfa Aesar, 99.95%), and which was then irradiated for 6 h using a 400 W Xe arc-lamp with constant stirring using a magnetic stir bar. UV-Vis measurements of the remaining solution confirmed a complete deposition of the platinum cocatalyst. After platinization, the particles were separated via centrifugation, washed with deionized water to remove any remaining Cl^- ions, and then dried overnight in an oven at 80°C. For the photocatalytic H_2 measurements, 150 mg of the platinized $PbTiO_3$ was then added to the fused-silica reaction vessel and filled with 20% aqueous methanol solution. The added methanol functions as a hole scavenger, thereby generating CO_2 from its photo-oxidation, and which allows the measurement of the H_2 formation rate alone without the typically more difficult concomitant formation of O_2 being necessary and potentially rate limiting.³² The net balanced reaction is: $CH_3OH + H_2O \rightarrow 3 H_2 + CO_2$. For the photooxidation of H_2O to O_2 , each sample was first loaded with a 1 wt% RuO_2 cocatalyst via incipient wetness impregnation, as described before.^{5,33} For photocatalytic O_2 measurements, 150 mg of the loaded $PbTiO_3$ was then added to the fused-silica reaction vessel and filled with a 0.1 M $AgNO_3$ solution. The sacrificial Ag^+ is reduced at the $PbTiO_3$ surface to Ag metal under irradiation, which allows the formation of O_2 alone. The net balanced reaction is: $2 AgNO_3 + H_2O \rightarrow 2 Ag_{(s)} + 2 HNO_3 + 1/2 O_2$. Further details of these photocatalytic measurements have been described previously.²⁰

III. Results and Discussion

The $PbTiO_3$ solid crystallizes in a distorted perovskite structure-type in the tetragonal space group $P4mm$ and is a well-known ferroelectric.³⁴ The TiO_6 octahedra are condensed via corner sharing while Pb atoms occupy the interstitial sites. The PXRD pattern of the flux products, shown in Fig. 1, could be fitted and

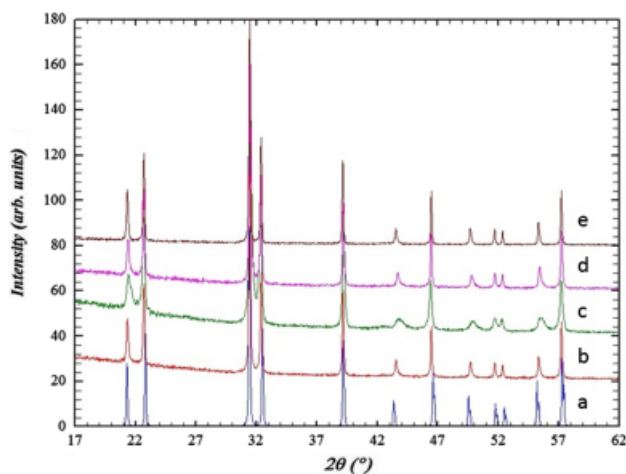


Fig. 1. The powder X-ray diffraction (PXRD) patterns of the $PbTiO_3$ products. (a) Calculated theoretical $PbTiO_3$ pattern, (b) solid-state method (c) 1:1 NaCl Flux heated for 1 h, (d) 10:1 NaCl flux heated for 1 h, (e) 2:1 PbO flux heated for 1 h.

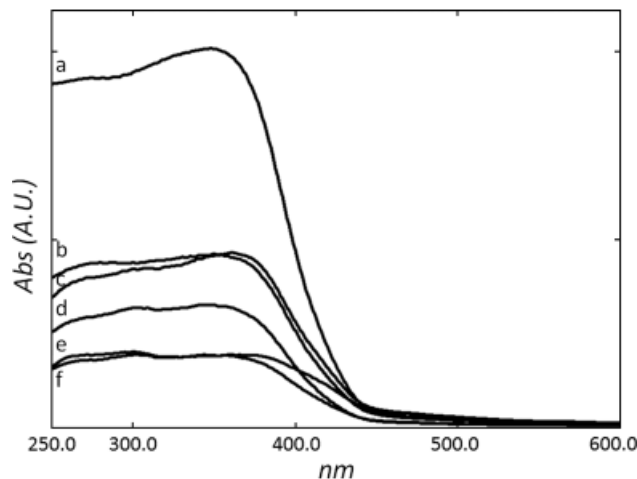


Fig. 2. UV-Vis diffuse reflectance spectra of $PbTiO_3$ powders prepared via (a) solid-state methods, (b) 1:1 NaCl (PBO1), (c) 0.5:1 PbO (PBO4), (d) 1:1 PbO (PBO5), (e) 20:1 NaCl (PBO3), and (f) 10:1 NaCl (PBO2). Reflectance has been converted to absorbance by the Kubelka-Munk method.

indexed to the reported $PbTiO_3$ structure, confirming that high purity and good crystallinity could be obtained in only a 1 h reaction time within molten NaCl and PbO fluxes at flux: $PbTiO_3$ molar ratios of 0.5:1, 1:1, 10:1, and 20:1. Refined unit-cell parameters for all samples were calculated using the LATCON program reporting the following lattice range ($a = 3.9018$ – 3.9081 Å) and ($c = 4.134$ – 4.154 Å).³⁰ The NaCl salt was selected as a flux based on previous successful reports, as well as its low cost and ease of removal after the reaction.²⁹ The PbO flux was chosen owing to its common ion and sufficiently low melting point. The excess loaded PbO flux was easily subsequently removed upon washing with 1M HNO_3 . An EDX analysis was also performed on $PbTiO_3$ samples in order to confirm the elemental compositions and revealed Pb, Ti, and O in approximately the 1:1:3 molar ratio. There was no significant detection of any Na^+ , indicating the NaCl flux had been removed completely by washing. Measurements of the UV-Vis DRS were taken on all $PbTiO_3$ samples in order to determine their optical bandgap sizes, and are shown for several selected samples in Fig. 2. In all cases, the bandgap size was calculated to be within a range of ~ 2.72 – 2.78 eV based on the onset of absorption, and which was found to be consistent with previous reports.¹⁷

Field-emission scanning electron microscopic (FESEM) images were taken on several $PbTiO_3$ samples in order to evaluate their particle sizes and morphologies. Figure 3 shows $PbTiO_3$ particles prepared using a 1:1 NaCl flux (Figs 3a and b) and a 10:1 NaCl flux (Figs 3c and d). Both samples reveal small, roughly spherical-like particles that fuse into larger aggregates. A distribution of particle sizes was observed, with the edge dimensions of the particles ranging from ~ 100 to 250 nm for the 1:1 NaCl flux-prepared samples and ~ 75 to 180 nm for the 10:1 NaCl flux-prepared samples. An estimation of the average particle sizes was made based on size measurements of ~ 20 randomly selected particles that were observed in different regions of the sample. These measurements for the 1:1 NaCl flux prepared samples yield average sizes of ~ 170 nm while those prepared with a 10:1 NaCl flux yielded an average size of ~ 130 nm. The FESEM images of the PbO flux-prepared samples are shown in Figure 4 and reveal a contrasting morphology, with particles forming large rectangular and cube-like structures with sizes ranging from ~ 1000 to 10 000 nm. Figure 4(b) shows at higher magnification the particle surfaces exhibit small domains with 90° step edges. For comparison, images were also taken of $PbTiO_3$ samples prepared by the traditional solid-state method, shown in Fig. 5. The solid-state products were observed to be small poly-faceted particles with little distinctly well-defined morphology and rougher surface features compared with those

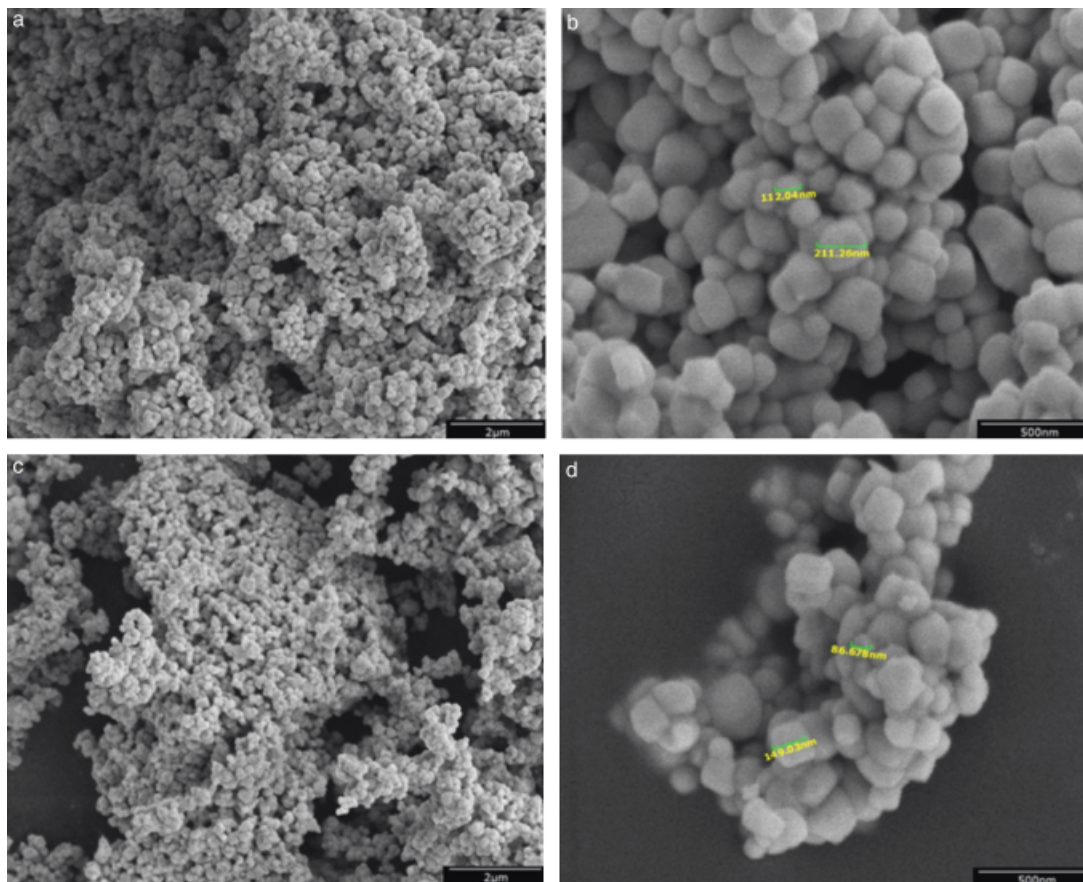


Fig. 3. Field-emission scanning electron microscopic (FESEM) images of (a, b) PBO1 and (c, d) PBO2 prepared at 1000°C for 1 h using a NaCl molten flux in flux: PbTiO_3 ratios of (a, b) 1:1 and (c, d) 10:1

prepared using the NaCl flux. The average size of the particles was estimated to be ~ 400 nm.

The FESEM images were also taken for selected samples that were photodeposited with 1% (wt.) platinum cocatalyst. Upon irradiation of light with energy greater than the bandgap of PbTiO_3 , nanosized Pt particles can be photodeposited onto the surface of the semiconductor particles. The locations of the photodeposited Pt particles can serve as a probe to understand where the most photocatalytically active surfaces of the particles occur. The 20:1 NaCl flux-prepared PbTiO_3 is shown in Fig. 6 both before (a and b) and after (c and d) the platinum photodeposition. The platinum particles deposit onto the surface as approximately 15 nm islands, and are in general uniformly dis-

tributed among the different surfaces of the spherical particles. The deposition of Pt onto the surface of PbTiO_3 prepared using a 1:1 NaCl flux is shown in Fig. 7, and reveals small Pt islands deposited in a similar fashion to those observed for the samples prepared in a 20:1 NaCl flux. For comparison, the platinized solid-state sample is shown in Fig 7b. Although Pt nano-islands were found in several areas of the particles' surfaces, particularly high concentrations of Pt deposits were observed along edges, grooves, and rough areas of the particle. It has been shown that platinum will preferentially photodeposit onto the most active sites of a metal oxide photocatalyst.^{35,36} It is likely that these areas of the PbTiO_3 particles are the most active surface sites, and therefore received the highest density of Pt deposits. The

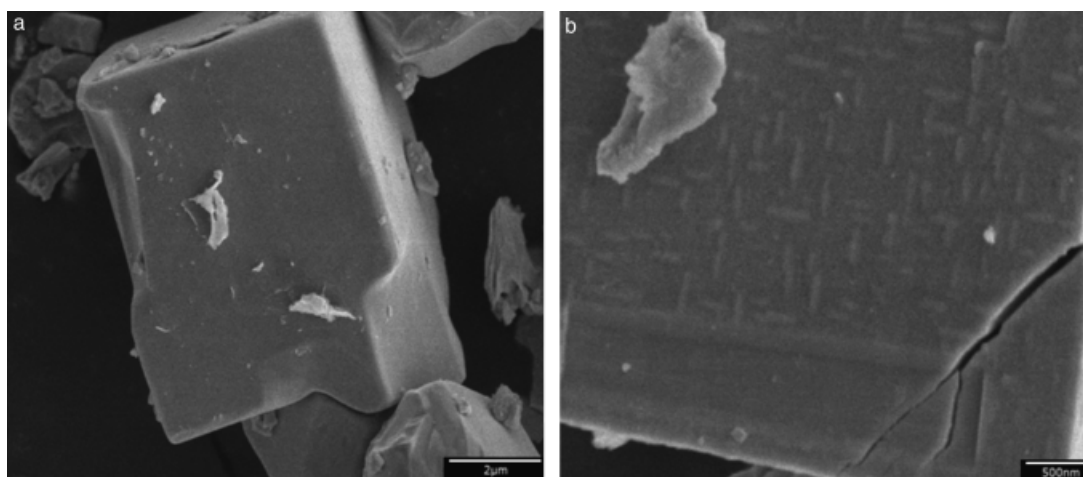


Fig. 4. Field-emission scanning electron microscopic (FESEM) images of PBO6 prepared at 1000°C for 1 h in a PbO molten flux with a flux: PbTiO_3 molar ratio of 2:1.

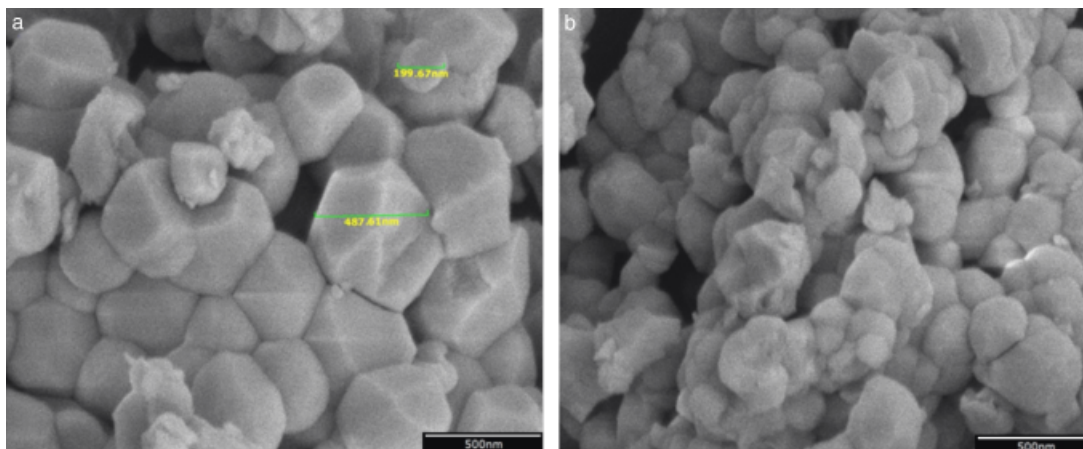


Fig. 5. Field-emission scanning electron microscopic (FESEM) images of the solid-state PbTiO_3 prepared at 1000°C for 48 h.

NaCl flux-prepared samples were roughly spherical with few surface features, and resulted in a rather uniform distribution of Pt deposition over the particles' surfaces.

Surface area measurements were performed on several powdered PbTiO_3 samples and their average values are listed in Table I. For the NaCl-flux samples the surface area generally increased upon increasing the amount of flux used in the reaction. This trend is consistent with the observed particle sizes from the FESEM images. The samples with the highest average surface area of $2.65 \text{ m}^2 \cdot \text{g}^{-1}$ were the 10:1 NaCl flux-prepared particles (PBO2). The 20:1 NaCl flux samples (PBO3) yielded an average of $2.36 \text{ m}^2 \cdot \text{g}^{-1}$, which indicates that the particle size modulation by the flux had reached a maximum limit. For the PbO flux reactions, the surface area varied from $0.56 \text{ m}^2 \cdot \text{g}^{-1}$ for the 0.5:1 PbO flux (PBO4) to $1.08 \text{ m}^2 \cdot \text{g}^{-1}$ for the 1:1 PbO flux

(PBO5) to $0.39 \text{ m}^2 \cdot \text{g}^{-1}$ for the 2:1 PbO flux (PBO6). This suggests that use of PbO as a flux is less effective at yielding small particle sizes as compared with the NaCl flux, which showed a more linear correlation. For comparison, the PbTiO_3 products prepared by the solid-state method (PBO std.) exhibited a surface area of $0.46 \text{ m}^2 \cdot \text{g}^{-1}$, and which is lower in surface area than any samples prepared using the NaCl flux, but comparable to the PbTiO_3 samples prepared using the smallest amount of PbO flux (PBO4).

The PbTiO_3 particles prepared by solid-state methods have previously been shown to both oxidize water to O_2 and to reduce water to H_2 using sacrificial reagents under visible irradiation.¹⁷ To observe the photocatalytic water-splitting reactions, irradiated photons of bandgap or greater energies must excite electrons in a semiconductor to create electron/hole pairs, which can

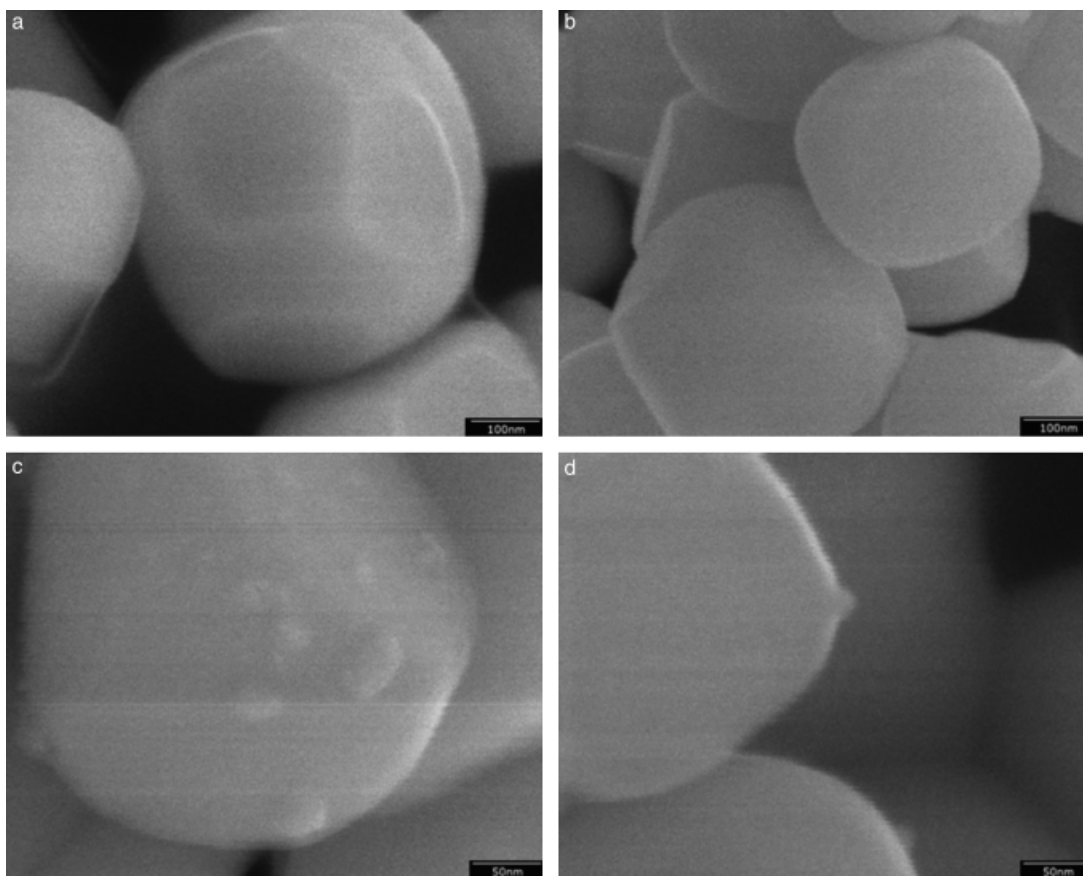


Fig. 6. Field-emission scanning electron microscopic (FESEM) images of PBO3 prepared in a 20:1 NaCl flux showing (a and b) bare particles before platinum photodeposition and (c and d) with a 1% wt. Pt photodeposited cocatalyst.

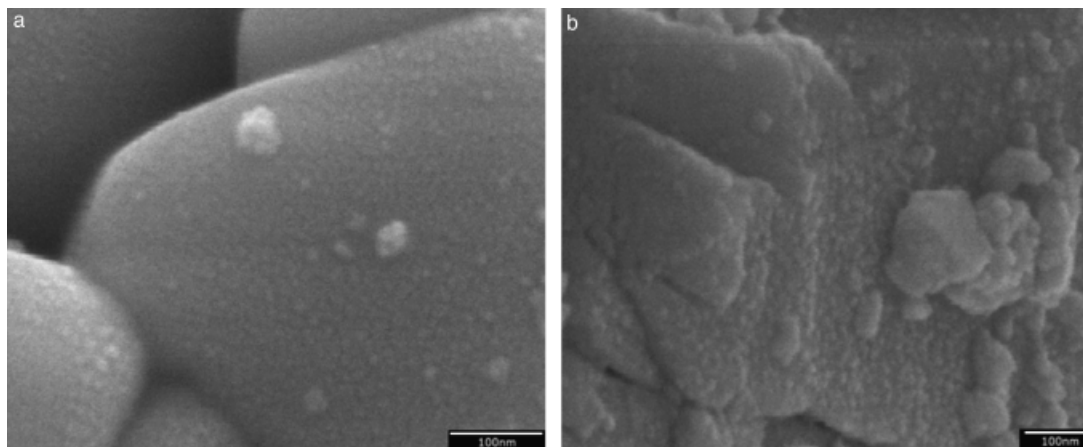


Fig. 7. Field-emission scanning electron microscopic (FESEM) images of platinumized PbTiO_3 prepared (a) using a 1:1 NaCl Flux (PBO1) and (b) by traditional solid-state methods (PBO std.).

then both oxidize and reduce water into O_2 and H_2 , respectively. In these experiments, AgNO_3 and CH_3OH were employed as sacrificial reagents to observe both half reactions separately. The flux syntheses of different particle sizes and morphologies should impact the rates of these reactions. The photocatalytic rates of H_2 and O_2 production for the flux-prepared PbTiO_3 products are given in Table I. The rate of O_2 formation decreased over time due to metallic silver being deposited onto the surface of the particles and effectively passivating the surface from further reaction. Therefore, the initial activity rate was regarded as the rate of reaction.³⁷ The rates of H_2 formation under visible irradiation were very low compared with the rates observed for O_2 . Therefore, the H_2 producing reactions were carried out under ultraviolet irradiation (>300 nm), while the O_2 producing reactions were performed under visible irradiation (>420 nm). An aqueous solution of 20% MeOH with no added catalyst yielded no production of H_2 under UV irradiation, thereby showing that all the H_2 gas produced in the reactions are from the activity of the PbTiO_3 catalysts and not from any possible methanol photolysis. In general for the NaCl flux-prepared reactions, the rates of O_2 and H_2 evolution decreased with increasing surface area and smaller particle sizes, which were obtained by increasing the amount of flux used during synthesis. The highest observed rate of O_2 from the NaCl flux prepared samples was $155.8 \mu\text{mol} \cdot \text{O}_2 \cdot (\text{g} \cdot \text{h})^{-1}$ for the PbTiO_3 particles prepared from the 1:1 NaCl flux, while for H_2 production the sample from the 20:1 NaCl flux evolved at the highest rate of $25.3 \mu\text{mol} \cdot \text{H}_2 \cdot (\text{g} \cdot \text{h})^{-1}$. The 10:1 NaCl flux sample, which also had the highest observed surface area, recorded the lowest rates for both O_2 and H_2 production, yielding $81.5 \mu\text{mol} \cdot \text{O}_2 \cdot (\text{g} \cdot \text{h})^{-1}$ and $2.8 \mu\text{mol} \cdot \text{H}_2 \cdot (\text{g} \cdot \text{h})^{-1}$, respectively. In all NaCl-prepared

samples, the activity was observed for at least 24 h. For the PbO flux-prepared samples, the observed photocatalytic activities were quite similar, with the 1:1 PbO flux sample showing slightly higher rates of activity for both O_2 and H_2 production. When compared with the NaCl flux samples, the PbO flux-prepared particles yielded higher rates of activity in all cases, suggesting that activity is not dependent upon having a large surface area or small particle sizes. For comparison, the photocatalytic rates of O_2 and H_2 evolution of the solid-state prepared PbTiO_3 were $183.1 \mu\text{mol} \cdot \text{O}_2 \cdot (\text{g} \cdot \text{h})^{-1}$ and $19.9 \mu\text{mol} \cdot \text{O}_2 \cdot (\text{g} \cdot \text{h})^{-1}$, respectively. These rates were higher than all NaCl flux-prepared samples, while at the same time exhibiting lower surface area and larger particle sizes from SEM observations. The activity was similar, however, to the observed rates for both PbO flux-prepared samples (PBO4 and PBO5), which had comparable surface areas. This is most likely due to the solid state and PbO flux-prepared samples having a greater amount of active surfaces for photocatalytic O_2 and H_2 evolution.

In general, particle size has been shown to have a significant impact on the photocatalytic activity, with the smaller particle sizes generally exhibiting higher photocatalytic rates.^{19,38} However, this relationship is in contrast to our observed rates for PbTiO_3 . The SEM images of the PbO flux-prepared samples show small nano-sized features at the surface of the particles that are not observed on any images taken of the NaCl flux-prepared samples. Similarly, the SEM images of the solid-state prepared samples show rough-edged particles with grooves that when photodeposited with a Pt cocatalyst received a higher concentration of Pt islands than in other areas of the particle. The NaCl flux-prepared particles were the smallest particles observed, but their surface features are quite smooth with relatively

Table I. Measured photocatalytic rates of O_2 and H_2 formation for flux-prepared PbTiO_3 and also for its solid-state method

Sample	Flux:AgNbO ₃ Ratio	Cocatalyst (1% wt.)	Wavelength (nm)	Surface Area (m ² g ⁻¹)	Activity ($\mu\text{mol} \cdot \text{O}_2 \cdot$ (g · h) ⁻¹)	Activity ($\mu\text{mol} \cdot \text{H}_2 \cdot$ (g · h) ⁻¹)
PbTiO_3 std*	–	RuO ₂	>420	0.46	183.1	–
		Pt	>300			19.9
PBO1	1:1 NaCl	RuO ₂	>420	1.43	155.8	–
		Pt	>300			9.1
PBO2	10:1 NaCl	RuO ₂	>420	2.63	81.5	–
		Pt	>300			2.8
PBO3	20:1 NaCl	RuO ₂	>420	2.36	143.4	–
		Pt	>300			25.3
PBO4	0.5:1 PbO	RuO ₂	>420	0.56	172.3	–
		Pt	>300			27.0
PBO5	1:1 PbO	RuO ₂	>420	1.08	180.7	–
		Pt	>300			27.4

*Prepared by solid-state reaction of PbO and TiO₂ reactants at 1000 C for 48 h. Testing Conditions: Outer irradiation 1000 W high-pressure Xe arc-lamp, 150 mg of PbTiO_3 , 20% MeOH_(aq) or 0.08M AgNO_{3(aq)}, and 1 wt% Pt or RuO₂ surface cocatalyst.

few observable surface features and showed no preferential Pt deposition sites. The photocatalytic rates of PbTiO₃ particles with these more terraced surface features and edges were the highest observed, while samples that did not exhibit these features (i.e. the NaCl flux-prepared samples) were less active. Platinum deposition has also previously been shown to preferentially deposit onto the {110} surface of TiO₂ particles, indicating that specific exposed faces aid in electron/hole separation during the photocatalytic reaction.³⁹ Also, several studies have shown that the dipolar fields in ferroelectric materials can more efficiently separate charge carriers and reduce recombination, thereby increasing photocatalytic activity.^{40–43} Given that the ferroelectric polarization is diminished in nanosized particles, this effect may explain the decreased activity observed in the smallest PbTiO₃ particles.²⁹ It has also been reported for NaTaO₃, that La-doping yields nano-stepped surface features that dramatically increase photocatalytic activity by creating separate surface sites for the formation of O₂ and H₂.^{10,44} Thus, a combination of the larger particle sizes and the nano-features and edges observed in PbTiO₃ lead to its highest observed photocatalytic activities.

IV. Conclusions

The visibly-active PbTiO₃ can be prepared in either a NaCl or PbO flux, yielding high purities and homogeneous microstructures that range in size from ~100 to 10000 nm, with the highest surface areas obtained for the 10:1 NaCl flux-prepared samples. Optical characterization revealed bandgap sizes of the PbTiO₃ products in the range of ~2.72–2.78 eV, which produced visible-light photocatalytic rates of 81.5–180.7 μmol·O₂·(g·h)⁻¹ and ultraviolet photocatalytic rates of 2.8–27.4 μmol·H₂·(g·h)⁻¹ in sacrificial AgNO₃ and MeOH solutions, respectively. Higher rates were correlated with the formation of surface nano-features with distinct edges and grooves on the PbO flux-prepared particles. By comparison, the PbTiO₃ sample prepared by the solid-state method also exhibited rough particle surfaces, yet little well-defined particle morphology. Thus, the results demonstrate the value of flux synthetic methods in tuning particle sizes and surface microstructures in order to probe the origins of photocatalytic activity on the surfaces of metal-oxide particles.

Acknowledgments

Financial support of this research is acknowledged from the Chemical Sciences, Geosciences and Biosciences Division, Office of Basic Energy Sciences, Office of Science, U.S. Department of Energy (DE-FG02-07ER15914).

References

- Fujishima and K. Honda, "Electrochemical Photolysis of Water at a Semiconductor Electrode," *Nature*, **238** [5358] 37–8 (1972).
- Domen, J. Kondo, M. Hara, and T. Takata, "Photo- and Mechano-Catalytic Overall Water Splitting Reactions to Form Hydrogen and Oxygen on Heterogeneous Catalysts," *Bull. Chem. Soc. Jpn.*, **73** [6] 1307–31 (2000).
- Domen, M. Hara, J. Kondo, T. Takata, A. Kudo, H. Kobayashi, and Y. Inoue, "New aspects of Heterogeneous Photocatalysts for Water Decomposition," *Kor. J. Chem. Eng.*, **18** [6] 862–6 (2001).
- D. W. Hwang, H. G. Kim, J. S. Lee, J. Kim, W. Li, and S. H. Oh, "Photocatalytic Hydrogen Production from Water over M-Doped La₂Ti₂O₇ (M = Cr, Fe) under Visible Light Irradiation," *J. Phys. Chem. B*, **109** [6] 2093–102 (2005).
- H. Kato, K. Asakura, and A. Kudo, "Highly Efficient Water Splitting into H₂ and O₂ over Lanthanum-Doped NaTaO₃ Photocatalysts with High Crystallinity and Surface Nanostructure," *J. Am. Chem. Soc.*, **125** [10] 3082–9 (2003).
- D. W. Hwang, G. H. Kim, J. S. Jang, S. W. Bae, S. M. Ji, and J. S. Lee, "Photocatalytic Decomposition of Water-Methanol Solution over Metal-Doped Layered Perovskites under Visible Light Irradiation," *Catal. Today*, **93** [93–95] 845–50 (2004).
- H. Kato, H. Kobayashi, and A. Kudo, "Role of Ag⁺ in the Band Structures and Photocatalytic Properties of AgMO₃ (M:Ta and Nb) with the Perovskite Structure," *J. Phys. Chem. B*, **106** [48] 12441–7 (2002).
- S. Kohtani, N. Yamamoto, K. Kitajima, A. Kudo, H. Kato, K. Tokumura, K. Hayakawa, and R. Nakagaki, "Photodegradation of 4-n-Nonylphenol and Natural Estrogens using Heterogeneous Visible-Light-Driven AgNbO₃ or BiVO₄ Photocatalyst," *Photo/Electrochem. Photobiol. Environ., Energy Fuel*, **173** [184] 173–84 (2004).

- R. Kenta, H. Kato, H. Kobayashi, and A. Kudo, "Photophysical Properties and Photocatalytic Activities under Visible Light Irradiation of Silver Vanadates," *Phys. Chem. Chem. Phys.*, **5** [14] 3061–5 (2003).
- A. Kudo, H. Kato, and I. Tsuji, "Strategies for the Development of Visible-Light-Driven Photocatalysts for Water Splitting," *Chem. Lett.*, **33** [12] 1534–9 (2004).
- K. Maeda, K. Teramura, D. Lu, N. Saito, Y. Inoue, and K. Domen, "Roles of Rh/Cr₂O₃ (Core/Shell) Nanoparticles Photodeposited on Visible-Light-Responsive (Ga_{1-x}Zn_x)(Ni_{1-x}O_x) Solid Solutions in Photocatalytic Overall Water Splitting," *J. Phys. Chem. C*, **111** [20] 7554–60 (2007).
- C. Zhang and Y. Zhu, "Synthesis of Square Bi₂WO₆ Nanoplates as High-Activity Visible-Light-Driven Photocatalysts," *Chem. Mater.*, **17** [13] 3537–45 (2005).
- J. Yoshimura, Y. Ebina, J. Kondo, K. Domen, and A. Tanaka, "Visible Light-Induced Photocatalytic Behavior of a Layered Perovskite-type Ruddigium Lead Niobate, RbPb₂Nb₃O₁₀," *J. Phys. Chem.*, **97** [9] 1970–3 (1993).
- T. Takata, K. Shinohara, A. Tanaka, M. Hara, J. Kondo, and K. Domen, "A Highly Active Photocatalyst for Overall Water Splitting with a Hydrated Layered Perovskite Structure," *J. Photochem. Photobiol. A, Chem.*, **106** [1–3] 45–9 (1997).
- Y. Inoue, Y. Asai, and K. Sato, "Photocatalysts with Tunnel Structures for Decomposition of water. Part 1. BaTi₄O₉, a Pentagonal Prism Tunnel Structure, and its Combination with Various Promoters," *J. Chem. Soc., Faraday Trans.*, **90** [5] 797–802 (1994).
- H. G. Kim, D. W. Hwang, and J. S. Lee, "An Undoped, Single-Phase Oxide Photocatalyst Working under Visible Light," *J. Am. Chem. Soc.*, **126** [29] 8912–3 (2004).
- H. G. Kim, O. S. Becker, J. S. Jang, S. M. Ji, P. H. Borse, and J. S. Lee, "A generic Method of Visible Light Sensitization for Perovskite-Related Layered Oxides: Substitution effect of lead," *J. Solid State Chem.*, **179** [4] 1214–8 (2006).
- D. G. Porob and P. A. Maggard, "Flux Syntheses of La-Doped NaTaO₃ and its Photocatalytic Activity," *J. Solid State Chem.*, **179** [6] 1727–32 (2006).
- D. Arney, B. Porter, B. Greve, and P. A. Maggard, "New Molten Salt Synthesis and Photocatalytic Properties of La₂Ti₂O₇ Particles," *J. Photochem. Photobiol. A, Chem.*, **199** [2–3] 230–5 (2008).
- D. Arney, C. Hardy, B. Greve, and P. A. Maggard, "Flux Synthesis of AgNbO₃: Effect of Particle Surfaces and Sizes on Photocatalytic Activity," *J. Photochem. Photobiol. A, Chem.*, **214**, 54–60 (2010).
- C. Chiu, C. Li, and S. B. Desu, "Molten Salt Synthesis of a Complex Perovskite, Pb(Fe_{0.5}Nb_{0.5})O₃," *J. Am. Ceram. Soc.*, **74** [1] 38–41 (1991).
- R. H. Arendt, "The Molten Salt Synthesis of Single Magnetic Domain BaFe₁₂O₁₉ and SrFe₁₂O₁₉ Crystals," *J. Solid State Chem.*, **8** [4] 339–47 (1973).
- R. H. Arendt, J. H. Rosolowski, and J. W. Szymaszek, "Lead Zirconate Titanate Ceramics from Molten salt Solvent Synthesized Powders," *Mater. Res. Bull.*, **14** [5] 703–9 (1979).
- D. B. Hedden, C. Torardi, and W. Zegarski, "M'-RTaO₄ synthesis: Activation of the precursor oxides by the reaction flux," *J. Solid State Chem.*, **118** [2] 419–21 (1995).
- M. A. El-Toni, S. Yin, and T. Sato, "Particle Size Control of plate-like Lepidocrocite-Related Potassium Lithium Titanate through Optimization of Synthesis Parameters," *Mater. Lett.*, **60** [2] 185–9 (2006).
- Y. Kan, X. Jin, P. Wang, Y. Li, Y.-B. Cheng, and D. Yan, "Anisotropic Grain Growth of Bi₄Ti₃O₁₂ in Molten Salt Fluxes," *Mater. Res. Bull.*, **38** [4] 567–76 (2003).
- D. G. Porob and P. A. Maggard, "Synthesis of Textured Bi₅Ti₃FeO₁₅ and LaBi₄Ti₃FeO₁₅ Ferroelectric Layered Aurivillius Phases by Molten-Salt Flux Methods," *Mater. Res. Bull.*, **41** [8] 1513–9 (2006).
- A. Aboujilil, J.-P. Deloume, F. Chassagneux, J.-P. Scharff, and B. Durand, "Molten Salt Synthesis of the Lead Titanate PbTiO₃. Investigation of the Reactivity of Various Titanium and Lead Salts with Molten Alkali-Metal Nitrites," *J. Mater. Chem.*, **8** [7] 1601–6 (1998).
- Z. Cai, X. Xing, R. Yu, X. Sun, and G. Liu, "Morphology-Controlled Synthesis of Lead Titanate Powders," *Inorg. Chem.*, **46** [18] 7423–7 (2007).
- D. Schwarzenbach, "Statistical Descriptors in Crystallography: Report of the International Union of Crystallography Subcommittee on Statistical Descriptors," *Acta Crystallogr., Sect. A: Found. Crystallogr.*, **A45**, 63–75 (1989).
- H. Nakamatsu, T. Kawai, A. Koreeda, and S. Kawai, "Electron-Microscopic Observation of Photodeposited Pt on TiO₂ Particles in Relation to Photocatalytic Activity," *J. Chem. Soc., Faraday Trans. 1: Phys. Chem. Condensed Phases*, **82** [2] 527–31 (1986).
- M.E. Graetzel, *Energy Resources Through Photochemistry and Catalysis*. Academic Press, New York, NY, 1983.
- Z. Zou and H. Arakawa, "Direct Water Splitting into H₂ and O₂ under Visible Light Irradiation with a New Series of Mixed Oxide Semiconductor Photocatalysts," *J. Photochem. Photobiol. A, Chem.*, **158** [2–3] 145–62 (2003).
- A. M. Glazer and S. A. Mabud, "Powder Profile Refinement of Lead Zirconate titanate at Several Temperatures. II. Pure Lead Titanate (PbTiO₃)," *Acta Crystallogr., Sect. B: Struct. Crystallogr. Crystal Chem.*, **B34** [4] 1065–70 (1978).
- Y. Matsumoto, S. Ida, and T. Inoue, "Photodeposition of Metal and Metal Oxide at the TiO_x Nanosheet to Observe the Photocatalytic Active Site," *J. Phys. Chem. C*, **112** [31] 11614–6 (2008).
- O. C. Compton, E. C. Carroll, J. Y. Kim, D. S. Larsen, and F. E. Osterloh, "Calcium Niobate Semiconductor Nanosheets as Catalysts for Photochemical Hydrogen Evolution from Water," *J. Phys. Chem. C*, **111** [40] 14589–92 (2007).
- A. Kudo, K. Omori, and H. Kato, "A Novel Aqueous Process for Preparation of Crystal Form-Controlled and Highly Crystalline BiVO₄ Powder from Layered Vanadates at Room Temperature and Its Photocatalytic and Photophysical Properties," *J. Am. Chem. Soc.*, **121** [49] 11459–67 (1999).
- A. Kudo and Y. Miseki, "Heterogeneous Photocatalyst Materials for Water Splitting," *Chem. Soc. Rev.*, **38** [1] 253–78 (2009).

³⁹T. Ohno, K. Sarukawa, and M. Matsumura, "Crystal Faces of Rutile and Anatase TiO_2 particles and their Roles in Photocatalytic Reactions," *New J. Chem.*, **26**, 1167–70 (2002).

⁴⁰J. L. Giocondi and G. S. Rohrer, "Spatial Separation of Photochemical Oxidation and Reduction Reactions on the Surface of Ferroelectric $BaTiO_3$," *J. Phys. Chem. B*, **105**, 8275–7 (2001).

⁴¹N. V. Burbure, P. A. Salvador, and G. S. Rohrer, "Influence of Dipolar Fields on the Photochemical Reactivity of Thin Titania Films on $BaTiO_3$ Substrates," *J. Am. Ceram. Soc.*, **89**, 2943–5 (2006).

⁴²J. L. Giocondi and G. S. Rohrer, "Spatially Selective Photochemical Reduction of Silver on the Surface of Ferroelectric Barium Titanate," *Chem. Mater.*, **13**, 241–2 (2001).

⁴³Y. Inoue, "Photocatalytic Water Splitting by RuO_2 -Loaded Metal Oxides and Nitrides with d0- and d10-Related Electronic Configurations," *Energy Environ. Sci.*, **2**, 364–86 (2009).

⁴⁴A. Kudo and H. Kato, "Effect of Lanthanide-Doping into $NaTaO_3$ Photocatalysts for Efficient Water Splitting," *Chem. Phys. Lett.*, **33** [5-6] 373 (2000). □